© 2005 The Chemical Society of Japan

Selected Paper

Enantiopreferential DNA Binding: $[\{(5,6\text{-dmp})_2Ru\}_2(\mu\text{-bpm})]^{4+}$ Induces a B-to-Z Conformational Change on DNA

Palanisamy Uma Maheswari, Venugopal Rajendiran, Mallayan Palaniandavar,* Ramakrishnan Parthasarathi, and Venkatesan Subramanian[1]

School of Chemistry, Bharathidasan University, Tiruchirappalli-620 024, Tamilnadu, India

[1]Chemical Laboratory, Central Leather Research Institute, Chennai-600 020, Tamilnadu, India

Received September 21, 2004; E-mail: palani51@sify.com

The dinuclear ruthenium(II) complex $[\{(5,6\text{-dmp})_2Ru\}_2(\mu\text{-bpm})]^{4+}$ (5,6-dmp = 5,6-dimethyl-1,10-phenanthroline; bpm = 2,2′-bipyrimidine) was synthesized and the *meso* ($\Delta\Lambda$) and *rac* ($\Delta\Delta$, $\Lambda\Lambda$) diastereoisomers separated using cation-exchange chromatography, and characterized using CHN analysis as well as UV–visible and ^{1}H NMR spectra. The *rac* form was interacted with calf thymus DNA (CT DNA) and certain selected dodecanucleotides, like poly $d(GC)_{12}$ and poly $d(AT)_{12}$ and the hexanucleotide $d(GTCGAC)_2$. Absorption, emission and circular dichroic spectral techniques, DNA melting studies and viscometry were used to monitor the interactions. Induced biphasic CD signals due to exciton coupling between dinuclear complexes bound on the DNA nanotemplate and the complexes free in solution were observed in the UV region. In contrast, the mononuclear analogue *rac*-$[Ru(5,6\text{-dmp})_2(bipy)]^{2+}$ did not show any biphasic CD signal upon an interaction with DNA under identical conditions. An increase in the ionic strength of the buffer and a decrease in the length of the DNA lowered the extent of exciton coupling. Also, the complex preferentially bound to GC, rather than the AT sequence, as revealed from the higher intensity of the biphasic CD signal for the former. An equilibrium dialysis experiment unambiquously revealed the preferential binding of $\Delta\Delta$-enantiomer to CT DNA, and also its potential, interestingly, to induce a B-to-Z conformational change on DNA. The latter was confirmed by the ^{31}P NMR spectra of poly $d(GC)_{12}$ bound to the dinuclear complex. A DNA binding model involving the partial insertion of one of the 5,6-dmp ligands of the large dinuclear complex ($\Delta\Delta$-enantiomer) between the DNA base pairs in the minor groove was suggested using molecular modeling; this model is preferred over one involving simple, electrostatic groove binding. This is supported by viscometry studies, which indicate an enhancement in the relative viscosity of CT DNA upon an interaction with the dinuclear complex.

The potential application of substitution-inert transition-metal complexes as stereoselective probes of nucleic acid structures and as possible antitumour agents has initiated vigorous and extensive interest over the past decade.[1] Thus, mononuclear ruthenium(II) complexes of polypyridyl ligands have attracted much attention due to a combination of easily constructed rigid structures spanning all three spatial dimensions and rich photophysical properties; however, knowledge about the nature of DNA interactions remain only modest, and their relatively weak non-covalent DNA interaction (K_b, $\sim 10^3$–10^4 M^{-1}) limits their application.[2] Very recently, certain dinuclear ruthenium(II) complexes have been synthesized as probes for DNA structure with an aim to enhance the DNA binding affinity.[3–5] Such positively charged dimetallic complexes can associate within the grooves of polyanionic DNA, with the binding further stabilized by a variety of intermolecular forces, such as van der Waals, hydrophobic and hydrogen bonding interactions, and by the removal of DNA-bound water molecules.[6] Also, they permit increased variation in the size and shape, leading to a tuning of the properties, and allowing the development of new DNA probe molecules. While the mononuclear complex $[Ru(bipy)_2(pztp)]^{2+}$ (bipy = 2,2′-bipyridine; pztp = 3-(pyrazin-2-yl)-as-triazino[5,6-f]1,10-phenanthroline) is reported to bind to DNA through intercalation, the bulky dinuclear analogue $[(bipy)_2Ru(pztp)Ru(bipy)_2]^{4+}$ binds weakly through an electrostatic interaction.[7] Further, a dinuclear complex bigger than a mononuclear analogue is expected not to interact well with DNA because of the smaller dimensions of the DNA grooves. Thus, the relatively bulky dinuclear complex $[\{Ru(phen)_2\}_2(\mu\text{-HAT})]^{4+}$ (HAT = 1,4,5,8,9,12-hexaazatriphenylene) has been found to bind only weakly with DNA; however, it binds to partially denatured DNA more strongly than it does with the standard duplex DNA, because the former contains a more open structure.[8] Additionally, if each ruthenium centre in a dinuclear complex is chiral, then a greater number of stereoisomers (and hence subtle changes in molecular shape) are available for use as stereochemical probes of nucleic acids. Upon interactions of the *rac* ($\Delta\Delta$ and $\Lambda\Lambda$) and *meso* ($\Delta\Lambda$) forms of the symmetrical complex $[\{Ru(Me_2bipy)_2\}_2(\mu\text{-bpm})]^{4+}$ (Me_2bipy = 4,4′-dimethyl-2,2′-bipyridine; bpm = 2,2′-bipyrimidine) with the dodecanucleotide $d(CAATCCGGATTG)_2$, the strongest intermolecular NOEs were observed between the dodecanucleotide and the $\Delta\Delta$-isomer in the minor groove.[9] It has been proposed that van der Waals interactions are important for the binding of the above complex through the minor groove; although the metal complex is relatively bulky, the major groove may still be too wide to allow close van der Waals interactions.[9] On the

Published on the web May 7, 2005; DOI 10.1246/bcsj.78.835

other hand, binding studies of the dinuclear ruthenium(II) complexes $\Delta\Delta$-$[\{Ru(Me_2bipy)_2\}_2(\mu\text{-bpm})]^{4+}$ and $\Delta\Delta$-$[\{Ru(bipy)_2\}(\mu\text{-bpm})\{Ru(Me_2bipy)_2\}]^{4+}$ (bipy = 2,2′-bipyridine) with the tridecanucleotide $d(CCGAGAATTCCGG)_2$ reveal the selective binding of the complexes at the adenine bulge site of the oligonucleotide in the minor groove.[10] Thus, non-intercalating dinuclear complexes have been suggested to be excellent diagnostic agents for DNA bulged sequences with more open structures. Very recently, a dinuclear complex with two DNA binding moieties, linked by a flexible chain so as to enable the centers to interact independently, has been reported to bind strongly to DNA, in contrast to the above-mentioned dinuclear complexes.[11]

From our laboratory we very recently reported that the ammonia co-ligands of $[Ru(NH_3)_4(diimine)]^{2+}$ complexes (diimine = differently (di/tetra)methyl-substituted and modified 1,10-phenanthrolines) are possibly involved in a hydrogen-bonding interaction with calf thymus (CT) DNA, and that the 5,6-dimethyl-1,10-phenanthroline (5,6-dmp) complex is involved in an enhanced hydrophobic interaction with CT DNA.[12,13] Also, we observed that *rac*-$[Ru(5,6\text{-dmp})_3]^{2+}$ binds to CT DNA with an affinity much higher than that of the analogous 1,10-phenanthroline (phen) complex.[14] In contrast, both the Δ and Λ enantiomers of $[Ru(5,6\text{-dmp})_3]^{2+}$ were isolated, and interacted with several synthetic polynucleotides, showing that they switch off specific groove binding.[15] In fact, the 5,6-dimethyl substituted *N*-methyl-1,10-phenanthrolinium cation, among unsubstituted and other methyl-substituted *N*-methyl-phenanthrolinium cations, exhibits the highest DNA binding affinity.[16] Among several methyl-substituted and unsubstituted $[Os(phen)_3]^{2+}$ complexes, the 5,6-dmp complex displays a high DNA binding affinity.[17] Interestingly, $[Cu(5,6\text{-dmp})_2]^{2+}$ was shown to induce irreversible a B-to-Z conformational change through minor groove binding.[18] Again, in a DNA-fiber EPR study of the ternary copper(II) complexes of 1,10-phenanthrolines and amino acids, the intercalative binding of the complexes was found to be promoted by 5,6-dimethyl substitution on a phen ring.[19] In the present investigation, the new dinuclear *rac*-$[\{(5,6\text{-dmp})_2Ru\}_2(\mu\text{-bpm})]^{4+}$ complex containing symmetric bpm bridge (Fig. 1) was isolated, and the nature and extent of DNA binding and binding geometries and stereospecific interaction, if any, of the complex with CT DNA and certain selected synthetic polynucleotides were probed, with an aim to understand the effect of 5,6-dimethyl substitutents on DNA binding. Interestingly, the $\Delta\Delta$-enantiomer of the complex bound enantiopreferentially, inducing a B-to-Z conformational change on DNA, which was confirmed through CD and ^{31}P NMR spectral studies. Molecular-modeling studies suggest the binding of the complex in the minor groove, with one of the 5,6-dmp ligands partially inserted between the DNA base pairs supported by close van der Waals interactions.

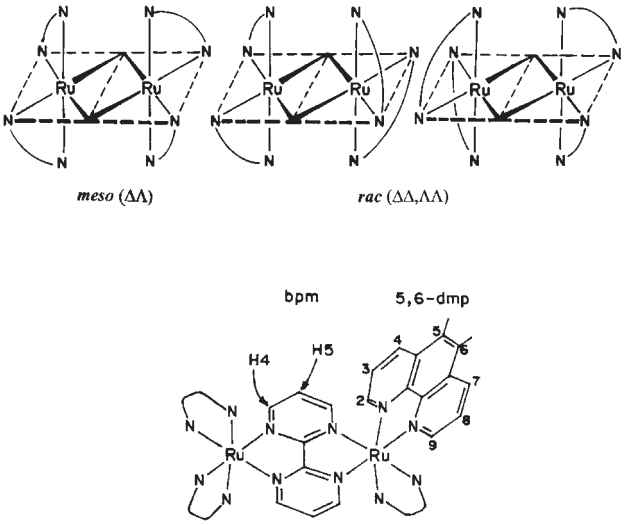

Fig. 1. Schematic view of the isomeric possibilities for $[\{Ru(5,6\text{-dmp})_2Ru\}_2(bpm)]^{4+}$.

Experimental

Materials. The self-complementary oligonucleotides $d(GC)_{12}$, $d(AT)_{12}$, and $d(GTCGAC)_2$ were purchased from The Microsynth GMB, Switzerland and stored at −20 °C. The concentrations of the oligonucleotides were calculated by measuring the OD at 260 nm for $d(GC)_{12}$ (ε, 8400), $d(AT)_{12}$, and $d(GTCGAC)_2$ (ε, 6600). $RuCl_3 \cdot 3H_2O$ was purchased from Arora Mathey limited. 5,6-Dimethyl-1,10-phenanthroline, SP Sephadex C-25, sodium 4-toluenesulfonate, and Amberlite IRA 400 were purchased from Aldrich Chemicals. 2,2′-bipyrimidine was purchased from Lanchaster. Disodium salt of calf thymus DNA (highly polymerized), purchased from Sigma, was stored at 4 °C and used as received. Ultra-pure Milli Q water (18.2 mΩ) was used in all experiments. Solutions of DNA in buffer, 50 mM NaCl/5 mM Tris HCl in water, gave a ratio of UV absorbance at 260 and 280 nm, A_{260}/A_{280}, of 1.9, indicating that the DNA was sufficiently free of protein.[20] Concentrated stock solutions of DNA (10.5 mM) were prepared in a buffer and sonicated for 25 cycles, where each cycle consisted of 30 sec with 1 min intervals. The concentration of DNA in nucleotide phosphate (NP) was determined by the UV absorbance at 260 nm after 1:100 dilutions. The extinction coefficient, ε_{260}, was taken as 6600 $M^{-1}\,cm^{-1}$. Stock solutions were stored at 4 °C and used after no more than 4 days.

Synthesis of the Complex. The precursor complex $[Ru(5,6\text{-dmp})_2Cl_2]$ was synthesized using a procedure reported for the synthesis of $[Ru(bipy)_2Cl_2]$.[21] $RuCl_3 \cdot 3H_2O$ (1 mmol) and 5,6-dmp (2 mmol) were refluxed overnight in DMF with 50% excess LiCl. After refluxing, cold acetone was added to the solution and was cooled at 0 °C for at least 7 h. The obtained precipitate was washed well with H_2O to reduce the $[Ru(5,6\text{-dmp})_3]Cl_2$ formed simultaneously. After thorough washing, $[Ru(5,6\text{-dmp})_2Cl_2]$ was finally washed with diethyl ether and dried. Further, the above dark-brown product was purified using a Sephadex LH 20 column with CH_3CN/Toluene (3:1; v/v). Synthesis of the dinuclear complex was achieved using a procedure reported in the literature for $[\{Ru(Me_2bipy)_2\}_2(\mu\text{-bpm})]^{4+}$ (Me_2bipy = 4,4′-dimethyl-2,2′-bipyridine; bpm = 2,2′-bipyrimidine).[22,23] Bipyrimidine (bpm) (0.5 mmol) and $[Ru(5,6\text{-dmp})_2Cl_2]$ (1 mmol) were suspended in a 10% aqueous ethylene glycol solution (20 mL), and the mixture refluxed at approximately 120 °C for 5 hours.[22–24] The product was purified using cation-exchange chromatography (SP Sephadex C-25; eluent 0.2 M NaCl). Upon elution with 0.2 M NaCl, the first red band was removed and discarded. The second green band was eluted with a 0.5 M NaCl solution. A dark-green material was extracted with dichloromethane after the addition of a saturated solution of KPF_6; the solid was collected by vacuum filtration and washed with water. The complex was converted into the chloride salt by stirring a suspension with an anion-exchange resin

Amberlite IRA-400 column, and separated into diasteroisomers using cation-exchange column (dimensions $26 \times 1000\ mm^2$) chromatography SP Sephadex C-25; eluent 0.2 M sodium 4-toluenesulfonate) and were dried over P_2O_5. Bands 1 and 2 were determined to be the *meso*- and racemic (*rac*-) diastereoisomers, respectively, from NMR studies and by a comparison with other dinuclear complexes reported in the literature[22–24] (cf. below). Both eluent bands were extracted with dichloromethane, and the organic extracts dried with anhydrous Na_2SO_4. The addition of a saturated solution of KPF_6 yielded a precipitate, which was then converted to chlorides by passing an aqueous solution of the precipitate down an Amberlite IRA-400 column. The products were filtered and washed with cold diethylether. ^{1}H NMR (D_2O) *meso*-Form δ 9.35 (d, 4H, $J = 4.2$ Hz), 8.85 (d, 4H, $J = 4.2$ Hz), 8.3 (d, 4H, $J = 4.2$ Hz), 8.15 (m, 4H), 7.85 (d, 4H, $J = 4.2$ Hz), 7.75 (d, 4H, $J = 4.2$ Hz), 7.64 (m, 4H), 7.45 (t, 2H, $J = 4.2$ Hz), 2.42 (s, 12H), 2.30 (s, 12H). *rac*-Form δ 8.95 (d, 4H, $J = 4.2$ Hz), 8.8 (d, 4H, $J = 4.2$ Hz), 8.3 (d, 4H, $J = 4.2$ Hz), 7.95 (m, 4H), 7.85 (d, 4H, $J = 4.2$ Hz), 7.7 (d, 4H, $J = 4.2$ Hz), 7.6 (m, 4H), 7.42 (t, 2H, $J = 4.2$ Hz), 2.39 (s, 12H), 2.26 (s, 12H). UV–vis (H_2O): λ (nm), (ε (M^{-1})): 615 (6506), 417 (30000), 290 (30309), 266 (157428), 248 (167140). Anal. Calcd for [{5,6-dmp)$_2$Ru}$_2$(μ-bpm)]Cl_4: C, 57.57; H, 4.08; N, 12.59%. Found: C, 57.50; H, 4.02; N, 12.52%.

Methods and Instrumentation. Absorbance: Absorption spectra were recorded on a Varian Cary 300 Bio UV–vis Spectrophotomer using cuvettes of 1 cm path length. For UV–vis spectral titrations, 3.0×10^{-5} M concentration of ruthenium solutions were used and calf thymus DNA was added in steps until R = 40. The MLCT bands were monitored to follow the interaction of the complex with CT DNA and self-complementary oligonucleotides.

Emission: Emission intensity measurements were carried out using a Jasco F-4500 spectrofluorimeter. Tris buffer was used as a blank to make preliminary adjustments. The excitation wavelength was fixed and the emission range was adjusted before measurements. All of the measurements were made at 25 °C in a thermostated cuvette holder with a 5 nm entrance slit and a 5 nm exit slit. For emission spectral titrations, a 3×10^{-5} M concentration of ruthenium solutions were used and calf thymus DNA was added at R = 30.

Circular Dichroism: Circular dichroic spectra of DNA were obtained by using a JASCO J-716 spectropolarimeter equipped with a peltier temperature control device. All experiments were made using a 1 cm path quartz cell, unless specified. Each CD spectrum was collected after averaging over at least 4 accumulations using a scan speed of 100 nm min^{-1} and a 1 s response time. Machine + cuvette baselines were subtracted, and the resulting spectrum zeroed 50 nm outside of the absorption bands. No equilibration time was allowed prior to collection of the spectrum. Equilibrium dialysis experiments were performed using a dialysis tube of 12000 KD. A 2 mL sample of calf thymus DNA was dialysed against 80 mL of buffer containing a ruthenium complex, and solutions were dialysed for 24 h with continuous agitation at 4 °C.

Thermal Denaturation: DNA melting experiments were carried out by monitoring the absorption (260 nm) of CT DNA (160 μM) at various temperatures in both the absence and presence of the complex at a 1:1 ratio with a ramp rate of 1 °C/min using a Varian Cary 300 Bio UV–vis Spectrophotomer with a Peltier arrangement.

Viscometry: For viscosity measurements the viscometer was thermostated at 25 °C in a constant-temperature bath. The concentration of DNA was 160 μM in NP and the flowtimes were determined with a digital timer (1/R = [Ru]/[NP] = 0.5).

NMR: ^{1}H NMR spectra of the complex were recorded on a JEOL ECA-500 MHz spectrometer in D_2O. DQF-COSY and NOESY experiments were accumulated using 2048 data points in t_2 for 256 t_1 values with a pulse repetition delay of 2 s. The mixing time for the NOESY experiment was around 700 ms to observe the NOE cross peaks at around 10 °C. The ^{1}H chemical shifts were relative to a trimethylsilane propionic acid (TSP) internal standard. ^{1}H decoupled ^{31}P spectra were collected at 202 MHz in a 500 MHz spectrometer. The chemical shifts were relative to the internal standard trimethyl phosphate (TMP). Typically, 3456 scans were collected and Fourier transformed with exponential multiplication. Typical samples contained 1 mM duplex, 0.75 mM ruthenium complex, 20 mM NaCl and 1 mM sodium cacodylate buffer (pH 7) in 0.5 mL of D_2O.

Molecular Modeling: Molecular modeling was performed on a Silicon Graphics O2 workstation using the Biosym Modeling package from Molecular Simulation Inc. (SanDiego, CA). The B-DNA systems chosen for the study were the dodecamer duplex of sequences $d(AT)_{12}$, $d(CGCGAATTCGCG)_2$, and $d(GC)_{12}$. Models of 12 mer nucleotides were constructed using the Biopolymer program of the Insight II package. The ruthenium complexes chosen for the molecular mechanical studies with DNA were constructed using coordinates from the Insight II library. The metal complexes and each metal/B-DNA complex were subjected to minimization using Extensible Systematic Force Field (ESFF)[25] with a non-bonded cutoff of 10 Å and a sigmoidal distant-dependent dielectric function ($\varepsilon = 4r_{ij}$), which had been demonstrated to be an appropriate implicit treatment for the dielectric function in computing the electrostatic potential of nucleic acid. The energy minimization employed the steepest descent followed by conjugate gradient algorithms until the convergence criterion was reached. The geometry of the whole complex was then refined until convergence (criterion of Root Mean Square (RMS) energy gradient of 0.05 kcal/(mol Å)) was reached throughout. The B-conformation of the DNA was maintained when the calculation converged to the minimum energy. The interaction energies of Ru–DNA complexes could be estimated by calculating the difference between their total energies and the sum of lowest energies found for the optimized structures of free DNA and dinuclear complex. The negative of the interaction energy is the binding energy:

$$\text{I.E} = \text{T.E} - (\text{Sum of the individual energy}) = -\text{I.E} = \text{B.E},$$

where I.E is the interaction energy, T.E is the total energy of DNA/complex, and B.E is the binding energy.[26]

Results and Discussion

Synthesis and Characterization of Dimeric Complexes. A shiny dark green dinuclear complex was prepared by refluxing the bpm ligand with the precursor complex [Ru(5,6-dmp)$_2$Cl$_2$][21] in a 1:2 molar ratio in an aqueous ethyleneglycol medium. Purification and isomer separation were performed using an SP Sephadex C-25 cation-exchange column and sodium 4-toluenesulfonate as the eluent, as described in the literature.[22,23] CHN analysis data and 1D and 2D NMR spectral data (Supporting Information, Fig. S1, S2) were consistent with the formulation of the dinuclear complex as [{(5,6-dmp)$_2$Ru}$_2$(μ-bpm)]Cl_4.

An examination of the two diastereoisomeric forms of the dinuclear complexes show a significant difference in the relative orientations of the terminal ligands "above" and "below" the plane of the bridging ligand. In the present complex, where the bridging ligand is 2,2′-bipyrimidine, the "above plane" ligands are parallel in the $\Delta\Delta/\Lambda\Lambda$ (*racemic*) and are orthogonal in the $\Delta\Lambda/\Lambda\Delta$ (*meso*) diastereoisomers.[24,27] The purities of the two forms were checked by ^{1}H NMR spectroscopy (Supporting Information). The dinuclear complexes in which the two ruthenium centers have the same terminal ligands (5,6-dmp), the *racemic* ($\Delta\Delta/\Lambda\Lambda$) and the *meso* ($\Delta\Lambda$) forms have C_2 and C_i point-group symmetry, respectively.[24,27] In each case, the H2 to H9 protons of each 5,6-dmp ligand showed the normal coupling patterns, and assignments were made based on the COSY and NOESY connectivities. The H2 and H3 protons situated over the bridge showed the greatest differences in chemical shifts between the two isomers (~0.3 ppm), as previously observed for the other reported dinuclear complexes. Thus, they are very much shifted downfield for the *meso* isomer compared to those of the *racemic* isomer due to a greater anisotropic effect from the ring current of the adjacent 5,6-dmp ligand.[22,24,27] On the other hand, the H4 to H9 protons showed a smaller difference between the two diastereoisomers (~0.05 ppm). Accordingly, the first fraction was assigned as the *meso*, and the second as the *rac* diastereoisomer.

The dinuclear complex exhibits two bands in the visible region, one of which with a very high intensity (λ_{max}, 417 nm; ε_{max}, 30000 $M^{-1}\,cm^{-1}$) is assigned as Ru(II) $d\pi \rightarrow \pi^*$ (5,6-dmp) MLCT transition, while the other with low a intensity (λ_{max}, 612 nm; ε_{max}, 6510 $M^{-1}\,cm^{-1}$) is assigned as the Ru(II) $d\pi \rightarrow \pi^*$ (bpm) MLCT transition.[7,8] The bands in the UV region are due to intra-ligand $\pi \rightarrow \pi^*$ transitions of the 5,6-dmp (248 and 266 nm) and bpm (290 nm) ligands.[7–10] The complex $[Ru(5,6\text{-dmp})_2(bipy)]Cl_2$ is considered to be a mononuclear equivalent of the dinuclear complex for comparing the DNA binding properties.[14]

Absorption Spectral Studies. The electronic absorption spectra of the *rac*-dinuclear complex in the absence and presence of CT DNA (R = [NP]/[Ru complex] = 13) reveal hypochromism (19%) and a red-shift (3 nm) of the 417 nm MLCT band of the complex, which unambiquously reveals the strong association of the dinuclear complex with DNA (Fig. 2A, Table 1).[28] The observed hypochromism is higher than that (R = 40, 11%, no red-shift) for the mononuclear complex *rac*-$[Ru(5,6\text{-dmp})_2(bipy)]^{2+}$, suggesting that the mode and extent of DNA interaction of the dinuclear complex is different from the latter. Interestingly, at higher [NP]/[Ru complex] ratios an increase in absorbance leading to a plateau, where essentially 100% of the dinuclear complex is bound to the DNA, is observed (Fig. 2B). The hyperchromism is in sharp contrast to the uniform hypochromism observed for the mononuclear complex (Fig. 2B), and reflects the binding of the dinuclear complex molecules in the interior of the DNA and/or bridging of two DNA strands by the dinuclear complex, as more DNA binding sites become available (Fig. 3). A clear isosbestic point observed at 465 nm over the entire [NP]/[Ru complex] range up to and another one (470 nm) observed beyond R = 13 are consistent with the existence of two DNA binding regimes for the dinuclear complex. This is again in contrast to the monometallic complex, which displays only one isosbestic point. Obviously, the strong binding interaction between the tetrapositively charged dinuclear complex and the negatively charged polyanionic CT DNA is expected to be higher than the dipositively charged mononuclear analogue, as demonstrated by the higher hypochromicity observed for the former. No attempt was made to calculate the binding constant for the dinuclear complex because of the mixed spectral behaviour.

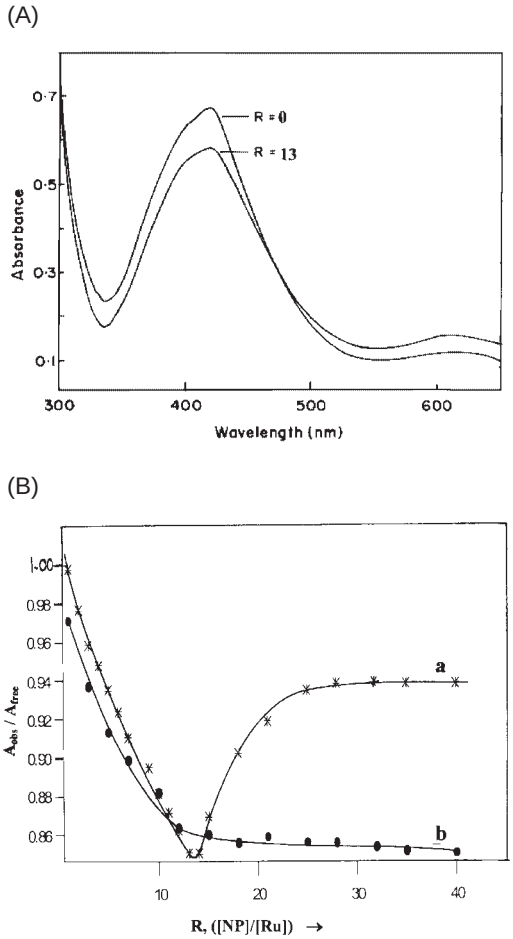

Fig. 2. (A) Absorption spectra of the dinuclear complex (3×10^{-5} M) in 5 mM Tris HCl buffer at pH 7.2 in the absence (R = 0) and presence (R = 13) of increasing amounts of DNA. (B) Absorption spectral changes observed upon addition of CT DNA (R = 0–40) to dinuclear (a) and mononuclear (b) complexes.

Table 1. Absorption Spectral Properties of the Dinuclear Complex on Binding to CT DNA and Polynucleotides

	Hypochromism	Red-shift
CT DNA	19%	3
	11%[a)]	—
Poly $d(GC)_{12}$	9%	2
Poly $d(AT)_{12}$	5%	—

Concentration of ruthenium solutions = 3×10^{-5} M. a) Binding parameters for the mononuclear complex with CT DNA.

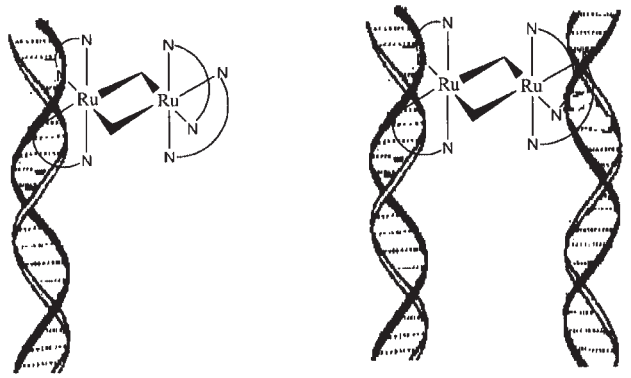

Fig. 3. Schematic representation of binding of [{(5,6-dmp)$_2$Ru}$_2$(μ-bpm)]$^{4+}$ to CT DNA in the minor groove at low (a) and high (b) concentrations of CT DNA.

The hypochromism and red-shift observed from the absorption spectral titrations of the dinuclear complex for interaction (R = 7) with the self-complementary polynucleotides d(GC)$_{12}$ (9%, 3 nm) and d(AT)$_{12}$ (5%, no red shift) are relatively low compared to CT DNA (Table 1). This reveals that CT DNA of a few hundred base pairs in length shows a stronger affinity for the cationic dinuclear complex. Interestingly, the absorption spectral change for the mixed sequence hexanucleotide is very small, revealing very weak affinity of the complex due to the decreased length of the polynucleotide.

Emission Spectral Studies. When the dinuclear complex was excited at its MLCT band (417 nm), a steady-state emission was observed at around 590 nm. The relative emission intensity of the complex increased ($I/I_0 = 1.2$, where I and I_0 are the emission intensities in the presence and absence of DNA, respectively) upon adding CT DNA (R = 5, 30), suggesting that the exciplex of the complex is protected from quenching by solvent molecules better in the hydrophobic environment of double-stranded DNA than in the aqueous environment (Supporting Information, Fig. S3).[29] The enhancement in the emission intensity ($I/I_0 = 1.2$; λ_{ex}, 450, λ_{em}, 590 nm) observed[14] for the mononuclear complex *rac*-[Ru(5,6-dmp)$_2$(bipy)]$^{2+}$ in the presence of DNA (R = 30) under identical conditions is the same as that for the dinuclear complex, supporting the above finding that both the di- and mononuclear complexes possess similar DNA binding environments at relatively higher [NP]/[Ru] mixing ratios.

Circular Dichroic Spectral Studies. Circular dichroic spectra provide information about the chirality of the spectroscopically active species in solution. They are particularly sensitive to the degenerate/non-degenerate exciton coupling expected to arise when the same/or two different chromophores are closely located in space to interact strongly.[30,31] The *rac* metal complexes give a zero CD, but may show induced circular dichroism (ICD) signals in the region of the intra-ligand and MLCT bands of the complexes upon DNA binding, (due to enantiopreferential binding and/or due to stereospecific perturbations, if any), providing a further and definitive confirmation for their DNA binding. Also, the CD spectral technique is useful for diagnosing changes in the DNA morphology during

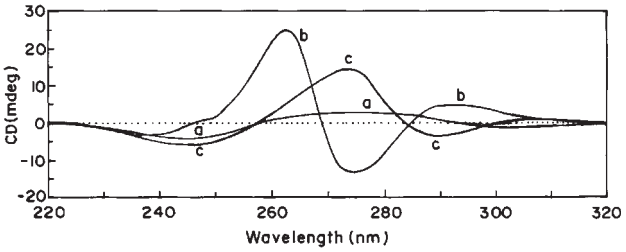

Fig. 4. Circular dichroism spectra of CT DNA in the absence (a) and presence of [{Ru(5,6-dmp)$_2$Ru}$_2$(bpm)]$^{4+}$ (b), and [Ru(5,6-dmp)$_2$(bipy)]$^{2+}$ (c) at 1/R value of 2; [DNA] = 2×10^{-6} M.

drug–DNA interactions, since CD signals are quite sensitive to the mode of the DNA interactions of small molecules. The changes in the CD signals of the DNA observed upon interactions with drugs may often be assigned to the corresponding changes in the DNA structure.[32,33] Further, the enantiopreferential binding of metal complexes can be clearly followed by using the CD bands.[34]

In the present study, each sample solution was scanned in the 220–320 nm region. A solution of CT DNA (2×10^{-6} M) exhibited a positive band (275 nm) due to base stacking and a negative band (248 nm) due to the right-handed helicity of DNA.[18] Upon interacting the DNA with the dinuclear complex (4×10^{-6} M, 1/R = [Ru complex]/[DNA] = 2), novel spectral features were discerned. The original negative and positive bands of CT DNA disappeared, and a new biphasic CD signal with positive (262 nm) and negative (274 nm) bands and an additional positive band at around 290 nm were observed with intensities much higher than that observed for free DNA (Fig. 4). Also, the zero cross-over point at 268 nm is consistent with the UV band maximum (266 nm) of the complex. The shape and intensity of the biphasic signal are typical of a CD signal arising from the exciton coupling between the chromophore of a DNA-bound dinuclear molecule with that of an unbound molecule in solution, and provide invaluable support for their strong binding to CT DNA. The induced CD at 290 nm would correspond to the π–π^* absorption band of a coordinated μ-bpm ligand of the DNA-bound complex. Thus, the DNA nanotemplate directs the bound complexes to form helical aggregates spontaneously so as to interact with each other through degenerate coupling. This type of exciton coupling was observed previously with certain organic dyes,[35] porphyrins[36] and copper–porphyrins[37] in the presence of DNA. It is also expected that the preferentially DNA-bound complex species are the $\Delta\Delta$-enantiomers (see below). The tendency of the complex to stack with each other, even in the unbound form, is evident from the absorbance vs [Ru complex] plot, which deviates from a straight line in the higher concentration range (2×10^{-6} to 2×10^{-4} M). The intensity of the biphasic CD signal is very high for low [NP]/[Ru complex] ratios (1/R = 2), that is, at high loadings of the dinuclear complex, where appreciable exciton coupling would take place, but decreases as the [NP]/[Ru complex] ratio (1/R = 0.1) is increased. This clearly reveals that the biphasic CD signal arises essentially when the DNA-bound/unbound complexes are stacked close to each other on the DNA nanotemplate (Supporting Information, Fig. S4). At higher [NP]/[Ru complex] ratios the binding

of the dinuclear complex is 100% when there will be less, or no, contact between the metal complexes, and hence less coupling is observed. Induced CD signals are also observed in the MLCT region with positive (402 nm) and negative (445 nm) components, increasing in intensity as the R value is increased from 5 to 40 (Supporting Information, Fig. S5). In contrast, for the mononuclear complex the biphasic signal does not arise upon an interaction with CT DNA under similar conditions, which reveals differences in the mode of DNA binding of the mono- and dinuclear complexes. Further, interestingly, the helicity band of CT DNA remained undisturbed when adding the mononuclear complex; however, the base stacking band was greatly disturbed with a blue shift (5 nm, Fig. 4). When ethidium bromide (EthBr) was added to DNA (R = 2) incubated with the dinuclear complex (R = 2), the biphasic CD signal in the UV region decreased in intensity. Obviously, the classical intercalator EthBr, which is known to bind avidly to DNA, displaces the bound metal complex, disturbs the DNA nanotemplate-promoted stacking of the complexes and results in a decrease in the exciton coupling (Fig. 5A). Upon adding EthBr to CT DNA (R = 2), the intensities of both the helicity and base stacking bands of the CT DNA increased due to the classical intercalation of EthBr, but when the dinuclear complex was added to this solution the intensities of both the bands decreased (Fig. 5B). Thus, both EthBr and the dinuclear complex compete for DNA binding and the CD signals observed in the presence of both EthBr and the complex is suggested to arise from a ternary complex–DNA–EthBr interaction.[38]

According to the polyelectrolyte theory[39] of Record et al., a study of the dependence of DNA binding of a complex on the sodium ion concentration would provide key information on the nature of DNA binding. The sensitivity of the extent of DNA binding to the ionic strength is expected to decrease in

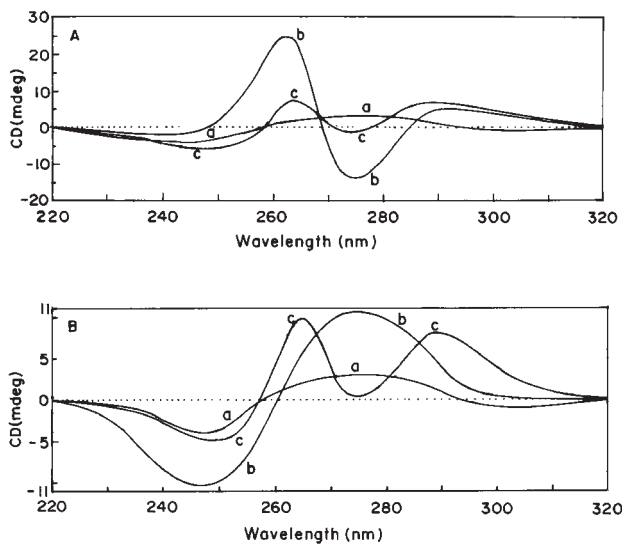

Fig. 5. (A) Circular dichroism spectra of CT DNA in the absence (a) and in the presence of dinuclear complex at R = 2 without (b) and with addition of EthBr at (R = 2) (c); [DNA] = 2×10^{-6} M. (B) Circular dichroism spectra of CT DNA in the absence (a) and in the presence of EthBr at R = 2 without (b) and with dinuclear complex (R = 2) (c); [DNA] = 2×10^{-6} M.

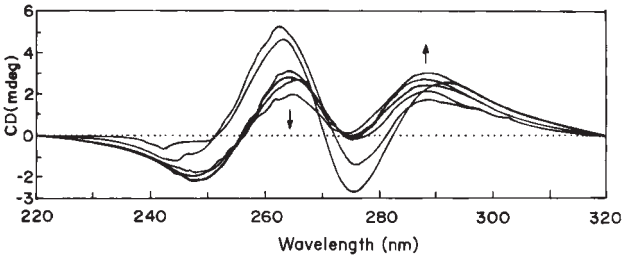

Fig. 6. Circular dichroism spectra of CT DNA in the presence of dinuclear complex (1/R = 2) at varying ionic strengths (0.05 to 2.5 M), cell length = 2 mm; [DNA] = 2×10^{-6} M.

the following order: electrostatic > groove binding > intercalative binding.[40] For the present dinuclear complex, when the ionic strength of the tris buffer was increased from 0.05 to 2.5 M using NaCl, both of the biphasic CD signals at 262 and 274 nm decreased in intensity, and finally a CD typical of B DNA appeared (Fig. 6). It is obvious that the increase in the Na^+ concentration in the Stern layer, which is known to stabilize the DNA backbone, decreases the binding affinity of the complex.[39] Thus, it is expected that the high-positively charged complex is involved in a strong electrostatic interaction with the polyanionic DNA, stabilized by an additional interaction, as illustrated above.

The interaction of the dinuclear complex (4×10^{-6} M) with the three oligonucleotides (poly $d(GC)_{12}$, poly $d(AT)_{12}$, and $d(GTCGAC)_2$) at 1/R = 2 leads to CD spectral features similar to those for CT DNA; however, differences in the CD intensities were observed, suggesting that the length and base sequences of the DNA are significant. Thus, interestingly, poly $d(GC)_{12}$ and poly $d(AT)_{12}$, both with 12 base pairs, show biphasic CD signal intensities higher than $d(GTCGAC)_2$ with only 6 base pairs, but much less than CT DNA with a few hundred base pairs of length (Fig. 7). Further, for poly $d(GC)_{12}$, the positive band at 290 nm dominates in intensity over the biphasic signal. Such a dependence of the intensity of CD signals upon the length of DNA is obviously because of the lesser number of adjacent polynucleotide-bound metal complexes involved in degenerate exciton coupling. The higher intensities of the biphasic signal for poly $d(GC)_{12}$ over poly $d(AT)_{12}$ confirms the preference of the dinuclear complex for binding to GC sequences, which is in conformity with the above absorption spectral results.

Equilibrium Dialysis. A solution of CT DNA (2.5 μM) was dialysed against a solution of the *rac* dinuclear complex (2.5 μM) for 24 h at 4 °C to study the enantiospecific interaction of the complex with DNA. The CD spectrum of the dialysate (Fig. 8) is similar to that of ΛΛ-enantiomers of other reported dinuclear complexes,[22] and is consistent with the presence of excess ΛΛ-enantiomer, revealing the enantiopreferential DNA binding of the ΔΔ-enantiomer. On the other hand, the CD spectrum of the retentate contains a positive band at around 260 nm and a negative band at around 290 nm (Fig. 8), which are quite different from those (a biphasic signal at 262 and 274 nm and a positive band at 290 nm) observed for CT DNA immediately after mixing it with the complex (cf. above). These CD features are akin to those observed for poly

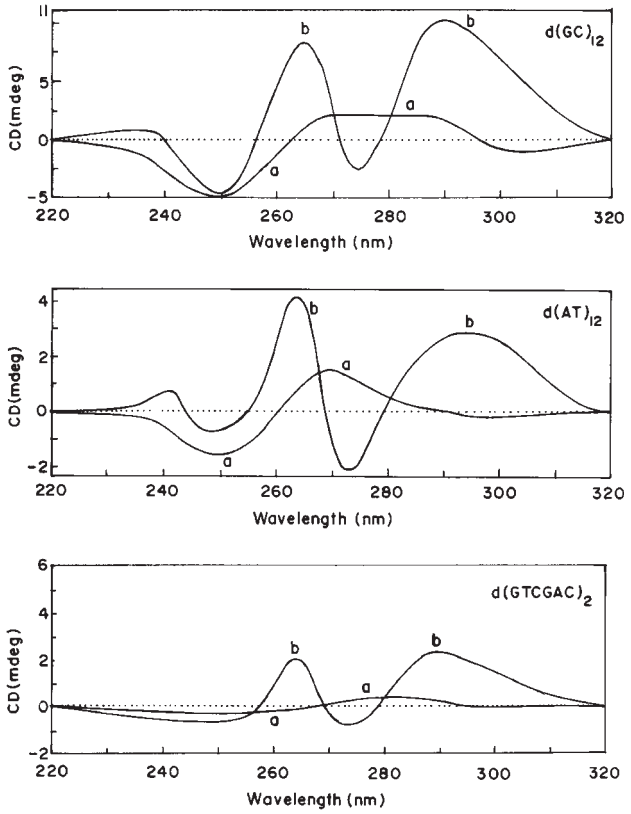

Fig. 7. Circular dichroism spectra of poly $d(GC)_{12}$, poly $d(AT)_{12}$, and $d(GTCGAC)_2$ in the absence (a) and presence of the dinuclear complex (b) ($1/R = 2$), Concentration of the polynucleotides $= 2 \times 10^{-6}$ M.

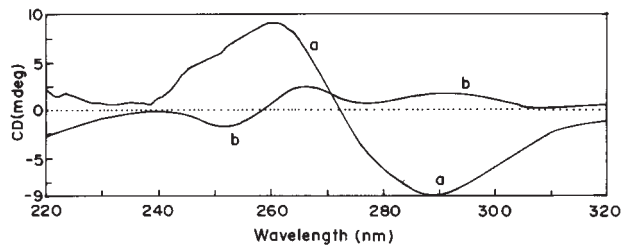

Fig. 8. Circular dichroism spectra of CT DNA (a) after dialysis against dinuclear complex for 24 h at 4 °C. The excess ΛΛ-enantiomer in the dialysate after 24 h dialysis (b); [DNA] $= 2.5 \times 10^{-6}$ M.

d(GC)·poly d(GC) at higher (5 M) NaCl concentrations at which the condition the Z form is stabilized.[41] Also, they are similar to those observed earlier for spermine, hexaamminecobalt(III), 85% ethanol and Ni^{2+} ions treated with poly(dG-dC)·poly(dG-dC) and for $[Cu(5,6\text{-dmp})_2]^{2+}$ bound to CT DNA.[42–46] Also, a negative CD band at around 197 nm and a shorter-wavelength cross over at around 185 nm were also discernible (Supporting Information, Fig. S6). Thus, the interesting spectral features observed upon treating CT DNA with the *rac*-form of the dinuclear complex are not certainly due to a simple overlap of the signals of CT DNA and the complex, but to signals induced upon interacting the complex with DNA and of the conformationally perturbed form of CT DNA. This is interesting because CT DNA with a low GC content is known to be not susceptible to the B-to-Z conformational change. However, the observation that poly $d(GC)_{12}$, which is well-known to stabilize the Z conformation, also displays CD signals (Supporting Information, Fig. S7) very similar to those displayed by CT DNA upon an interaction with the complex, supports the B-to-Z conformational change. In fact, it is also known that alternative GC stretches are not the only sequences capable of undergoing the B-to-Z transition, and thus even poly $d(AT)_{12}$ has been reported to stabilize the Z form.[47] Furthermore, when the above retentate was subjected again to dialysis against a 50 mM NaCl buffer solution (pH 7.1) for 2 h, the retentate yielded a CD spectrum with decreased intensity for both the positive and the negative CD bands typical of Z DNA. Upon continuing the dialysis for 10 more hours, the retentate yielded the original CD spectrum typical of natural B DNA, revealing that the conformational change is reversible. Thus, it is obvious from the dialysis experiments that the preferential binding of ΔΔ-isomer of the *rac*-complex occurs, resulting in a stabilization of the Z form on prolonged interaction. A variety of environmental conditions, including the presence of high salt concentrations,[41] transition metal complexes[48] and negative supercoiling[49] and chemical modifications, such as base bromination[50] and alkylation,[51] have been shown to strongly influence the B ⇌ Z equilibrium. We had previously observed[18] a similar B-to-Z trans conformational change upon the addition of $[Cu(5,6\text{-dmp})_2]^{2+}$ to CT DNA. The conformational change may be ascribed to the 5,6-dimethyl groups, which effectively place themselves between the phosphate groups at close proximity (5.9 Å)[52] with each other, leading to the potentiation of Z DNA by decreasing the repulsion otherwise present between them in Z DNA.[18] However, it is cautioned that the observed CD spectral changes may also be due to the formation of certain other forms of DNA, like a condensed form.

^{31}P NMR Spectral Study. In addition to the circular-dichroism technique, which is generally used for distinguishing between right-handed and left-handed DNA helices, the most useful are ^{31}P NMR chemical shifts and sugar protons, ^{1}H–^{1}H NOE, with the observation of an extremely short distance for purine nucleotides with a syn conformation in Z-DNA.[53] In B DNA the chemical-shift dispersion of the ^{31}P resonances is small, giving rise to a single, composite line. In contrast, for Z-DNA the conformational non-equivalence of the two phosphate groups in the dinucleotide repeat is reflected in distinctly different ^{31}P chemicals shifts.[54] The change in the hydrogen-decoupled ^{31}P NMR spectrum of poly $d(GC)_{12}$ (4.2 ppm) was followed to confirm the stabilization of Z-form DNA in the presence of the dinuclear complex. The two different phosphate signals (3.5 and 4.7 ppm) observed for poly $d(GC)_{12}$ dialysed against *rac*-$[\{(5,6\text{-dmp})_2Ru\}_2(\mu\text{-bpm})]^{4+}$ (Fig. 9) were similar to those observed for poly(dG-dC) at around 3 and 4.5 ppm on a salt-induced transition (6 M) from the B-to-Z conformation,[55] thus confirming stabilization of the Z-form DNA upon binding to the dinuclear complex.

Thermal Denaturation and Viscosity Studies. DNA melting-temperature studies are used to understand the nature of the interaction of complexes with CT DNA. The ΔT_m value of 7 ± 0.5 °C, obtained from a absorption vs temperature plot (Supporting Information, Fig. S8), is far less than that for a

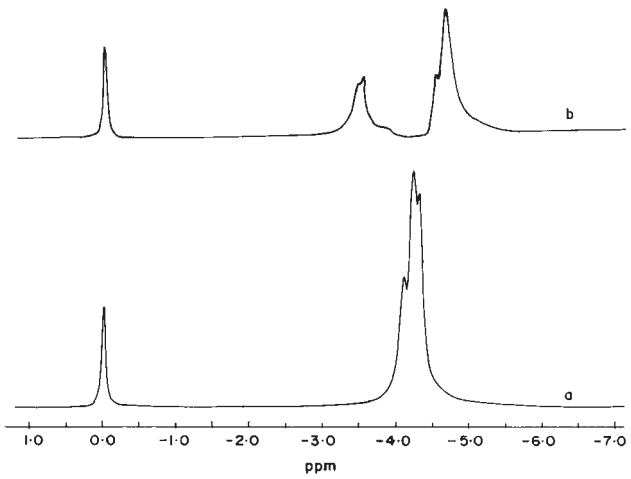

Fig. 9. Hydrogen decoupled ^{31}P NMR of poly d(GC)$_{12}$ in the absence (a) and in the presence of dinuclear complex (b).

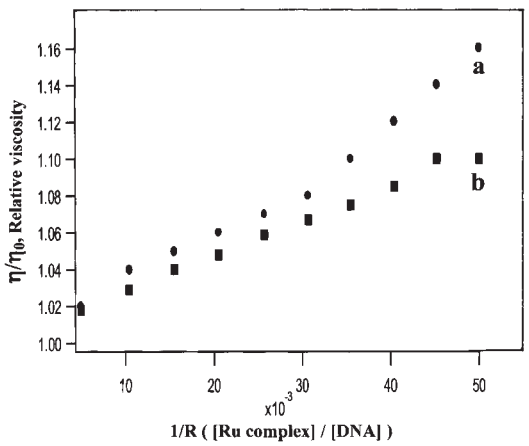

Fig. 10. The effect of the dinuclear complex (a), and [Ru(phen)$_3$]$^{2+}$ (b) on the viscosity of calf thymus DNA; Relative specific viscosity vs 1/R.

classical intercalator (ΔT_m = 10–14 °C),[56] but higher than the range for electrostatically bound complexes (ΔT_m = 1–2 °C).[57] Thus, the dinuclear complex is expected to involve in strong electrostatic binding, which is further supported by strong hydrophobic interactions of the 5,6-dimethyl substituted phenanthrolines, and stablize the double-stranded CT DNA.

Measuring the viscosity of DNA is a classical technique used to analyse the DNA binding mode in solution, and provides stronger evidence for the intercalative DNA binding mode. Viscosity measurements of CT DNA incubated with the dinuclear complex at a 1/R (= [Ru Complex]/[DNA]) value of 0.5 show an increase in the relative viscosity of CT DNA compared to [Ru(phen)$_3$]$^{2+}$,[58] which is known to increase the DNA viscosity through the partial insertion of a phen ring between the DNA base pairs (Fig. 10). It is evident that the 5,6-dimethyl groups do not hinder the phen ring from insertion between the base pairs. This is similar to the classical intercalator ethidium ion with its ethyl group perpendicular to the planar aromatic ring, encouraging the intercalation of EthBr, rather than hindering it.

Molecular Modeling. To obtain further support for the DNA-binding mode, the binding energies of the complex (ΔΔ-enantiomer) were calculated with different sequences, such as the Dickerson sequence, d(GCGCATATGCGC)$_2$, poly d(GC)$_{12}$, and poly d(AT)$_{12}$. Initially, the complex was manually docked at different sites of B-form DNA. Several starting geometries for intermolecular complexes were selected by a structure-based docking strategy and by considering all possible steric factors. After docking minimizations were performed on the intermolecular complexes to remove short contacts, short molecular dynamics were made to generate a variety of starting geometries. The results presented in this study are only for DNA–metal complexes that have a positive binding energy. It is evident from previous reports on the interaction of various Cr(III) complexes with DNA that Extensible Systematic Force Field (ESFF) provides reliable estimates of the binding energy, and a possible comparison with the experimental results can be rationalized.[25,26] Hence, in this study the binding energies for various modes of interaction of ruthenium complexes with DNA in the B conformation were computed (Table 2), which suggest that a partial insertion of one of the terminal 5,6-dmp ligands of the dinuclear complex through the minor groove is more favourable (Fig. 11). The energy for the binding of the metal complex with poly d(GC)$_{12}$ is much higher than that for poly d(AT)$_{12}$ in all modes of the interaction (Table 2), which is consistent with the better stacking interactions of the former polymer, as demonstrated by the above spectral studies. Upon binding of the dinuclear complex to poly d(GC)$_{12}$, the base pairs flanked with the distance increasing from 4.4 to 5.4 Å. However, the increase in the distance for the Dickerson sequence was less than that for poly d(GC)$_{12}$. The intercalation mode of interaction is not at all favourable for poly d(AT)$_{12}$; however, a major groove binding is favoured, in spite of the binding energy being less than that for the intercalation mode for the binding of poly d(GC)$_{12}$ and the Dickerson sequence. The double-helical structure of the polynucleotides in the B conformation is maintained upon metal complex binding. The root-mean-square deviation (RMSD), with respect to all atoms between the normal and interacted models, can be calculated by superimposing the normal and interacted models to gain insights on the changes of DNA upon metal complex binding. These values for the minor-groove intercalation for the Dickerson sequence, poly d(GC)$_{12}$ and poly d(AT)$_{12}$ have been found to be, respectively, 0.67, 0.98, and 0.60 Å with respect to all atoms. Based on this model a schematic representation of stacking of free and bound complex molecules is given in Fig. 12.

Table 2. Calculated Binding Energies of Dinuclear Complex (ΔΔ-Enantiomer) with Polynucleotides Through Molecular Modeling

	d(GC)$_{12}$	d(AT)$_{12}$	Dickerson
	B.E/kcal mol^{-1} a)	B.E/kcal mol^{-1}	B.E/kcal mol
Major Groove	40	22	35
Minor Groove	19	24	29
Intercalation/ Major Groove	25	22	28
Intercalation/ Minor Groove	66	07	25

a) Binding energy calculated.

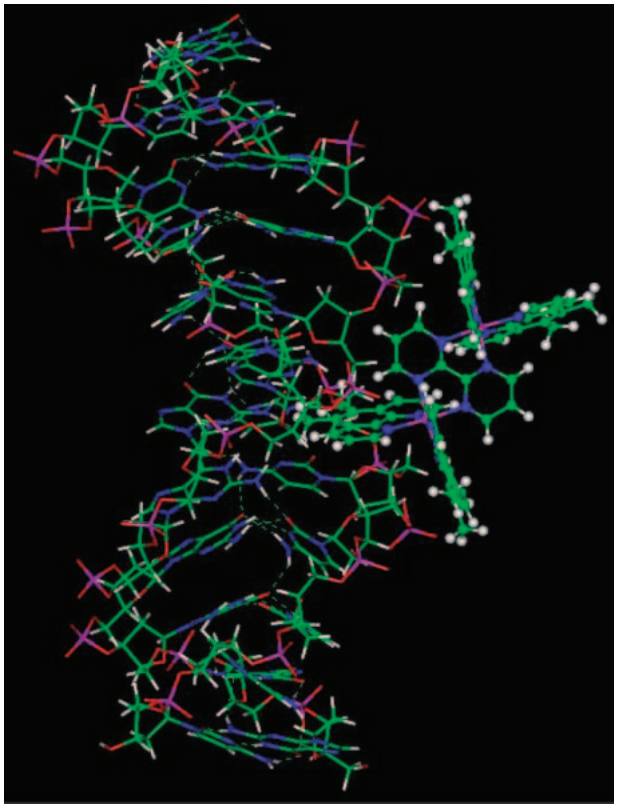

Fig. 11. Molecular model of ΔΔ-[{Ru(5,6-dmp)$_2$Ru}$_2$-(bpm)]$^{4+}$ bound to poly d(GC)$_{12}$ in the minor groove. (Generated using Insight II, Discover 3).

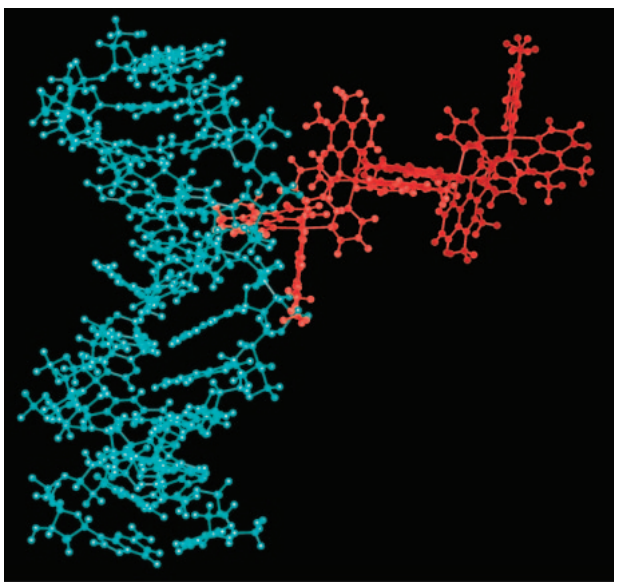

Fig. 12. Schematic view of stacking of ΔΔ-[{Ru(5,6-dmp)$_2$Ru}$_2$(bpm)]$^{4+}$ bound to poly d(GC)$_{12}$ in the minor groove. (Generated using Insight II, Discover 3).

Conclusion

The dinuclear complex *rac*-[{(5,6-dmp)$_2$Ru}$_2$(μ-bpm)]$^{4+}$ was found to bind strongly to CT DNA with a different binding mode and an affinity higher than that of an analogous mononuclear complex. A DNA binding model involving the electrostatic interaction of the tetracationic complex with the polyanionic DNA was suggested, which is supported by a partial insertion of the 5,6-dimethyl groups of the phenanthroline ring in the minor groove. Interestingly, induced CD signals observed in the UV region upon an interaction of the dinuclear complex with CT DNA and certain synthetic polynucleotides due to degenerate exciton coupling between the DNA-bound and unbound complexes also suggest a strong binding of the complex to DNA. Thus, the DNA nanotemplate directs the bound complexes to form helical aggregates spontaneously so as to interact with each other through degenerate coupling. Also, the intensity of the biphasic CD signal is DNA length and sequence dependent. Thus, it is of the highest intensity in CT DNA, low in polynucleotides, like poly d(GC)$_{12}$ and poly d(AT)$_{12}$, and less in the hexamer d(GTCGAC)$_2$. Further, the complex shows sequence specificity by predominantly binding to GC rather than to the AT sequence, as is evident from the absorption hypochromism, exciton coupled CD signals, and molecular modeling. The interesting results of an equilibrium dialysis experiment suggest a preferential binding of the ΔΔ-enantiomer to CT DNA, with the potential to bring about a B-to-Z conformational change on the DNA, as is evident from the ^{31}P NMR spectra of poly d(GC)$_{12}$ bound to the dinuclear complex.

The Board of Research in Nuclear Sciences, Department of Atomic Energy, Mumbai, is gratefully acknowledged for financial support (No. 2003/37/25/BRNS). Council of Scientific and Industrial Research, New Delhi is acknowledged for a Senior Research Fellowship to P. U. We thank Professor Raghavan Varadharajan, Molecular Biophysics Unit, Indian Institute of Science, Bangalore for providing CD spectral facility. Dr. T. Ramasami, Director and Mr. K. Victor Babu, Central Leather Research Institute, Chennai-600 020 are thanked for providing the NMR spectral facility.

Supporting Information

This material containing Figures S1–S8 is avilable free of charge on the web at http://www.csj.jp/journals/bcsj/.

References

1 K. E. Erkkila, D. T. Odom, and J. K. Barton, *Chem. Rev.*, **99**, 2777 (1999).

2 L. N. Ji, X. H. Zou, and J. G. Liu, *Coord. Chem. Rev.*, **216**, 513 (2001).

3 S. Komeda, M. Lutz, A. L. Spek, M. Chikuma, and J. Reedijk, *Inorg. Chem.*, **39**, 4230 (2000).

4 B. Onfelt, P. Lincoln, and B. Norden, *J. Am. Chem. Soc.*, **121**, 10846 (1999).

5 B. Onfelt, P. Lincoln, and B. Norden, *J. Am. Chem. Soc.*, **123**, 3630 (2001).

6 A. Brodkorb, A. K. Mesmaeker, T. J. Rutherford, and F. R. Keene, *Eur. J. Inorg. Chem.*, **2001**, 2151.

7 X. H. Zou, B. H. Ye, H. Li, J. G. liu, Y. Xiong, and L. N. Ji, *J. Chem. Soc., Dalton Trans.*, **1999**, 1423.

8 O. Van Gijte and A. K. Mesmaeker, *J. Chem. Soc., Dalton Trans.*, **1999**, 951.

9 F. M. Foley, F. R. Keene, and J. G. Collins, *J. Chem. Soc.,*

Dalton Trans., **2001**, 2968.
10 B. T. Patterson, J. G. Collins, F. M. Foley, and F. R. Keene, *J. Chem. Soc., Dalton Trans.*, **2002**, 4343.
11 F. M. O'Reilly and J. M. Kelly, *J. Phys. Chem. B*, **104**, 7206 (2000).
12 P. Uma Maheswari and M. Palaniandavar, *J. Inorg. Biochem.*, **2**, 219 (2004).
13 P. Uma Maheswari and M. Palaniandavar, *Inorg. Chim. Acta*, **357**, 901 (2004).
14 P. Uma Maheswari and M. Palaniandavar, unpublished results.
15 D. Z. M. Coggan, I. S. Haworth, P. J. Bates, A. Robinson, and A. Rodger, *Inorg. Chem.*, **38**, 4486 (1999).
16 E. J. Gabbay, R. E. Scofield, and C. S. Baxter, *J. Am. Chem. Soc.*, **95**, 7850 (1973).
17 K. Maruyama, J. Motonaka, Y. Mishima, Y. Matsuzaki, I. Nakabayashi, and Y. Nakabayashi, *Sens. Actuators, B*, **76**, 215 (2001).
18 S. Mahadevan and M. Palaniandavar, *Inorg. Chem.*, **37**, 3927 (1998).
19 M. Chikira, Y. Tomizawa, D. Fukita, T. Sugizaki, N. Sugawara, T. Yamazaki, A. Sasano, H. Shindo, M. Palaniandavar, and W. E. Antholine, *J. Inorg. Biochem.*, **89**, 163 (2002).
20 M. E. Reichmann, S. A. Rice, C. A. Thomas, and P. Poty, *J. Am. Chem. Soc.*, **76**, 3047 (1954).
21 B. P. Sullivan, D. J. Salmon, and T. J. Meyer, *Inorg. Chem.*, **40**, 5045 (2001).
22 F. R. Keene, *Chem. Soc. Rev.*, **27**, 185 (1998).
23 N. C. Fletcher and F. R. Keene, *J. Chem. Soc., Dalton Trans.*, **1999**, 683.
24 L. S. Kelso, D. A. Reitsma, and F. R. Keene, *Inorg. Chem.*, **35**, 5144 (1996).
25 S. Shi, L. Yan, and J. Fisher, "ESFF Forcefield Project Report II," MSI, Sandiego.
26 R. Vijayalakshmi, V. Subramanian, and B. Unni Nair, *J. Biomol. Struct. Dyn.*, **19**, 1 (2002).
27 N. C. Fletcher, P. C. Junk, D. A. Reitsma, and F. R. Keene, *J. Chem. Soc., Dalton Trans.*, **1998**, 133.
28 A. M. Pyle, J. P. Reymann, R. Meshoyrer, C. V. Kumar, N. J. Turro, and J. K. Barton, *J. Am. Chem. Soc.*, **111**, 3051 (1989).
29 J. K. Barton, J. M. Goldberg, C. V. Kumar, and N. J. Turro, *J. Am. Chem. Soc.*, **108**, 2081 (1986).
30 B. Norden and F. Tjerneld, *Biopolymers*, **21**, 1713 (1982).
31 J. L. Seifert, R. E. Connor, S. A. Kushon, M. Wang, and B. A. Armitage, *J. Am. Chem. Soc.*, **121**, 2987 (1999).
32 A. Rodger, B. Norden, P. M. Rodger, and P. J. Bates, *Eur. J. Inorg. Chem.*, **2002**, 49.
33 V. I. Ivanov, L. E. Minchenkova, A. K. Schyolkina, and A. I. Poletayev, *Biopolymers*, **12**, 89 (1973).
34 I. Meistermann, V. Moreno, M. J. Prieto, E. Moldrheim, E. Sletten, S. Khalid, P. M. Rodger, J. C. Peberdy, C. J. Isaac, A. Rodger, and M. J. Hannon, *PNAS*, **99**, 5069 (2002).
35 M. Wang, G. L. Silva, and B. A. Armitage, *J. Am. Chem. Soc.*, **122**, 9977 (2000).
36 L. G. Marzilli, G. Petho, M. Lin, M. S. Kim, and D. W. Dixon, *J. Am. Chem. Soc.*, **114**, 7575 (1992).
37 B. P. Hudson, J. Sou, D. J. Berger, and D. R. McMillin, *J. Am. Chem. Soc.*, **114**, 8997 (1992).
38 W. Muller and D. M. Crothers, *Biopolymers*, **35**, 251 (1968).
39 M. T. Record, T. M. Lohman, and P. J. De Haseth, *J. Mol. Biol.*, **107**, 145 (1976).
40 G. S. Q. Manning, *Rev. Biophys.*, **11**, 179 (1978).
41 F. M. Pohl and T. M. Jovin, *J. Mol. Biol.*, **67**, 375 (1972).
42 A. Parkinson, M. Hawken, M. Hall, K. J. Sanders, and A. Rodger, *Phys. Chem. Chem. Phys.*, **2**, 5469 (2000).
43 H. S. Basu and L. J. Marton, *Biochem. J.*, **244**, 243 (1987).
44 H. Robinson and A. H. J. Wang, *Nucleic Acids Res.*, **24**, 676 (1996).
45 T. Schoenknecht and H. Diebler, *J. Inorg. Biochem.*, **50**, 283 (1993).
46 P. Bourtayre, J. Liquier, L. Pzzorini, and E. Taillandier, *J. Biomol. Struct. Dyn.*, **5**, 97 (1987).
47 J. H. Riazance, W. A. Baase, W. C. Johnson, Jr., K. Hall, P. Cruz, and I. Tinoco, Jr., *Nucleic Acids Res.*, **13**, 4983 (1985).
48 P. S. Ho, C. A. Frederick, D. Saal, A. H. Wang, and A. Rich, *J. Biomol. Struct. Dyn.* **4**, 521 (1987).
49 C. K. Singleton, J. Klysik, S. M. Stirdivant, and R. D. Wells, *Nature*, **299**, 312 (1982).
50 A. Moller, A. Nordheim, S. A. Kozalowski, D. J. Patel, and A. Rich, *Biochemistry*, **23**, 54 (1984).
51 M. Behe and G. Felsenfeld, *Proc. Natl. Acad. Sci. U.S.A.*, **78**, 1619 (1981).
52 M. McCall, T. Brown, W. N. Hunter, and O. Kennard, *Nature*, **322**, 661 (1985).
53 J. Fegion, W. Leupin, W. A. Denny, and D. R. Kearns, *Biochemistry*, **22**, 5943 (1983).
54 D. J. Patel, S. A. Kozlowski, A. Nordheim, and A. Rich, *Proc. Natl. Acad. Sci. U.S.A.*, **79**, 1413 (1982).
55 T. A. Holak, P. N. Borer, G. C. Levy, J. H. van Boom, and A. H. Wang, *Nucleic Acids Res.*, **12**, 4625 (1984).
56 M. Cusumano and A. Giannetto, *J. Inorg. Biochem.*, **65**, 137 (1997).
57 E. Tsepi-Kalouli and N. Katsaros, *J. Inorg. Biochem.*, **37**, 271 (1989).
58 S. Satyanarayana, J. C. Dabrowiak, and J. B. Chaires, *Biochemistry*, **32**, 9319 (1992).